7.2 EFFECTS OF ION IRRADIATION ON BAM-11 BULK METALLIC GLASS

— A. G. Perez-Bergquist[1,2], *H. Bei[1], Y. Zhang[1,2], and S. J. Zinkle[1,2] (Oak Ridge National Laboratory[1], University of Tennessee[2])*

OBJECTIVE

The goal of this study is to investigate the radiation behavior of the bulk metallic glass BAM-11 and to determine if it is a viable candidate for high-radiation structural applications in fusion applications.

SUMMARY

Bulk metallic glasses are intriguing candidates for structural applications in nuclear environments due to their good mechanical properties along with their inherent amorphous nature, but their radiation response is largely unknown due to the relatively recent nature of innovations in bulk metallic glass fabrication. Here, microstructural and mechanical property evaluations have been performed on a $Zr_{52.5}Cu_{17.9}Ni_{14.6}Al_{10}Ti_5$ bulk metallic glass (BAM-11) irradiated with 3 MeV Ni^+ ions to 0.1 and 1.0 dpa at room temperature and 200°C. Transmission electron microscopy showed no evidence of radiation damage or crystallization following ion irradiation, and changes in hardness and Young's modulus were typically <10%, with slight softening following irradiation at room temperature and no significant changes at 200°C. These results suggest that the BAM-11 bulk metallic glass may be useful for certain applications in nuclear environments.

PROGRESS AND STATUS

Introduction

Amorphous metallic glasses were first synthesized in the 1960s [1] and have since received considerable scientific attention due to their appealing properties, including their good thermal conductivity, high strength, good ductility, and corrosion resistance [2-4]. In particular, metallic glasses are an intriguing candidate for use in radiation environments due to their lack of crystalline structure, which prohibits the formation of conventional radiation defects such as vacancy-interstitial Frenkel pairs and dislocation loops that occur in crystalline solids. Although particle irradiation can produce point defects and macroscopic changes in amorphous materials in a manner somewhat analogous to what happens in crystalline materials, there is some evidence that the amount of retained displacement damage can be significantly less in amorphous materials [5]. In addition, metallic glasses may possess high helium permeabilities due to their large free atomic volumes and lack of grain boundaries that can act as helium traps [5]. In fact, recent studies show that metallic glasses may be resistant to cavity swelling, and hence possibly tritium retention, as compared to crystalline materials, which would make them appealing for fusion energy applications [6].

Though metallic glasses could initially only be fabricated as thin sheets due to the extremely high cooling rates required to quench the material in the amorphous phase, pronounced advances have been made over the past few decades in metallic glass fabrication that now allow for the creation of high-performance structural glasses in bulk

form, thus vastly increasing their usefulness for structural applications [7,8]. To date, however, little data exists on the effects of displacement irradiation on these highly engineered metallic glasses. Different studies have reported crystallization of metallic glasses under irradiation [9-13] while others have not [6, 14-18], but tests have been performed on different amorphous alloys under different ion irradiation conditions and at varying temperatures (see Table 1). Though irradiation-induced softening has been reported in several studies [15, 18-20], and hardening has also been reported in at least one [11], mechanical properties of irradiated bulk metallic alloys are still largely unknown, as is the microstructural evolution of irradiated bulk metallic glasses as a function of irradiation dose and temperature.

Table 1. Summary of ion irradiation studies in bulk metallic glass, organized by incident ion fluence.

Material	Ion Species	Ion Energy (keV)	Ion Fluence (cm^{-2})	Temp.	Crystallization (Y/N)	Source
$Zr_{50}Cu_{40}Al_{10}$	Al^+, Xe^+	5000, 200000	1×10^{12} - 3×10^{14}	RT	N	[17,18]
$Zr_{55}Cu_{30}Al_{10}Ni_5$	Ga^+	30	7×10^{14} - 7×10^{15}	RT	N	[16]
$Ti_{40}Zr_{25}Be_{30}Cr_5$	C^+, Cl^+	2500	1×10^{15} - 8×10^{15}	LN	N	[15]
$Zr_{61.5}Cu_{21.5}Fe_5Al_{12}$	Ar^+	300	3×10^{15} - 3×10^{16}	RT	Y	[12]
$Ni_{52.5}Nb_{10}Zr_{15}Ti_{15}Pt_{7.5}$	Ni^+	1000	1×10^{16}	RT	Y	[13]
$Zr_{55}Cu_{30}Ni_5Al_{10}$	Co^+	40	7×10^{16}	140°C	N	[14]
$Fe_{81}B_{13.5}Si_{3.5}C_2$	He^+	2800	1×10^{16} - 1×10^{17}	RT	Y	[9]
$Cu_{50}Zr_{45}Ti_5$	He^+	140	1.7×10^{17}	RT	Y	[10]
$Zr_{55}Cu_{30}Al_{10}Ni_5$	Ar^+	10	2.7×10^{17}	RT	Y	[11]
$Cu_{47}Zr_{45}Al_8Y_{1.5}$	He^+	500	2×10^{17} - 2×10^{18}	-	N	[6]

Experimental Procedures

A $Zr_{52.5}Cu_{17.9}Ni_{14.6}Al_{10}Ti_5$ alloy (BAM-11) was fabricated by arc melting in an argon atmosphere using a mixture of base metals with the following purities: 99.5% Zr, 99.99% Cu, 99.99% Ni, 99.99% Al, and 99.99% Ti [21]. The alloy was then remelted and drop cast into a cylindrical copper mold of 7 mm in diameter in a Zr-gettered helium atmosphere. Sections of the drop cast rod were evaluated via x-ray diffraction (XRD) and differential scanning calorimetry, which both confirmed the material to be fully in the amorphous state. The rod was then cut into sections of 8 by 3 by 1 mm and mechanically polished to a mirror finish.

After fabrication, BAM-11 specimens were ion irradiated using 3 MeV Ni^+ ions at perpendicular incidence. Samples were implanted to fluences of 4.2×10^{13} and 4.2×10^{14} ions/cm^2, or peak damage levels of 0.1 and 1.0 dpa, respectively, at both room temperature and elevated temperature (200°C) at the University of Tennessee/ORNL Ion

Beam Materials Laboratory (IBML). Ion range and damage event profiles were used to determine the fluence to dpa conversion and were generated by the SRIM software using average displacement energy of 40 eV [22]. The mode of the ion range was calculated to be 1.36 μm, with implanted Ni concentrations reaching 5.5 x 10^{18} atoms/cm^3 at this depth. Damage levels at the sample surface were calculated be about 40% of peak levels. Elevated temperature irradiations were performed at 200°C to keep the metallic glass far below its glass transition temperature of 393°C [21].

Post-irradiation microstructural characterizations of the irradiated bulk metallic glass specimens were performed via transmission electron microscopy (TEM). TEM foils were fabricated using an FEI Quanta Dual-beam focused ion beam (FIB)/SEM with a final thinning step of 2kV Ga^+ ions at a glancing angle of about 4° in order to minimize ion beam milling damage. Samples were then analyzed in a Phillips CM 200 TEM operating at 200 kV using the techniques of bright field (BF) imaging, selected area electron diffraction (SAED), high resolution TEM (HRTEM), and x-ray energy dispersive spectroscopy (EDS) performed in scanning TEM (STEM) mode.

Mechanical properties were examined via microindentation using an MTS XP nanoindenter, with the indentations performed normal to the mechanically polished control and irradiated surfaces. All tests were performed using a Berkovitch diamond indenter (3 sided pyramidal tip) in continuous stiffness measurement mode at a constant indentation rate of 0.05/s with a maximum applied load of 200 mN [23]. For statistical purposes, each sample was indented a total of 16 times and the averages of those results are reported within this manuscript. Hardness and elastic modulus were measured as a function of depth from the point of contact of the nanoindenter with the surface to a depth of about 1200 nm. Data generated within the first ~100 nm of the surface was discarded due to large scatter associated with surface roughness.

Mechanical Properties

Hardness and elastic modulus data generated through nanoindentation tests were reported upon in the previous semiannual progress report (DOE/ER-0313/54 - Volume 54). However, due to concerns over surface finish of the tested samples, those measurements were retaken. Results of those experiments are shown in Figures 1 and 2.

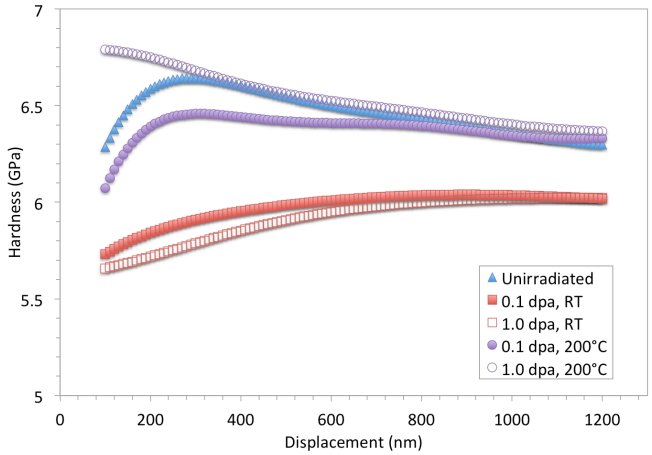

Figure 1. Hardness as a function of indenter depth in the unirradiated and irradiated BAM-11 specimens.

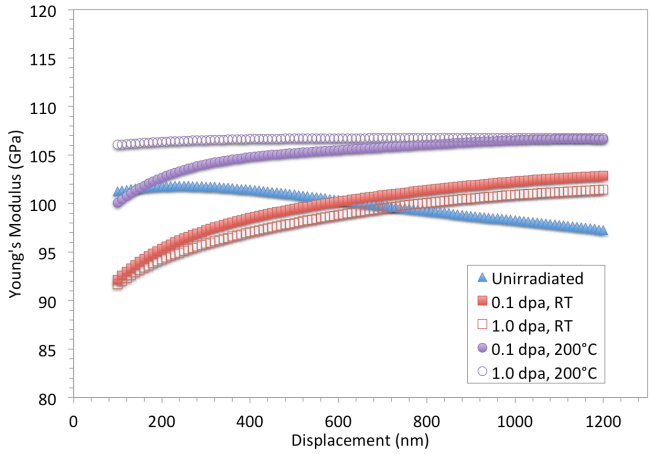

Figure 2. Elastic modulus as a function of indenter depth in the unirradiated and irradiated BAM-11 specimens.

Hardness and elastic modulus both dropped slightly for the specimens irradiated at room temperature as compared to the sample in the unirradiated condition. Hardness decreased about 12% from 6.6 GPa in the unirradiated state to 5.8 and 5.7 GPa in samples irradiated to 0.1 and 1.0 dpa at room temperature. Similarly, elastic modulus decreased about 7% from 101.8 GPa to 95.3 and 94.3 GPa, respectively.

In the samples irradiated at 200°C, the change in mechanical properties due to irradiation was even smaller than in the room temperature irradiations. Hardness in the samples irradiated at elevated temperature was relatively unchanged, with samples irradiated to 0.1 and 1.0 dpa exhibiting hardness values of 6.4 and 6.7 GPa. In addition, elastic modulus was seen to increase about 1-4% from 101.8 GPa in the unirradiated condition to 102.7 and 106.4 GPa in the samples irradiated to 0.1 and 1.0 dpa, respectively. Though data set variance was slightly higher for the samples irradiated at 200°C, the results

nonetheless seem to indicate a slightly better radiation tolerance of the bulk metallic glass at elevated temperature. Hardness remains unchanged at 200°C, likely due to somewhat enhanced self-annealing effects, and an increase in the Young's modulus, which is largely a function of interatomic bonding distance, suggests a slight densification of the BAM-11 alloy following irradiation.

Microstructure

Microstructural data derived via TEM, including BF imagery, SAED patterns, and HRTEM, was reported upon in detail in the previous semiannual progress report (DOE/ER-0313/54 - Volume 54) and will not be reiterated here. However, additional analysis has since been performed upon diffractograms of the HRTEM images taken from each specimen.

Fast Fourier transforms, also known as diffractograms, can provide insight into the atomic spacing of amorphous alloys. When a diffractogram is created from an image of an amorphous material, the result is a concentric ring pattern such as the one shown in Figure 3. The ratio of the distance between the primary circle at the center of the pattern and the surrounding rings can provide information as to the spacing of atoms in a material, and since a diffractogram is a representation of an image in reciprocal space, an expansion of diffractogram rings indicates material densification and vice versa. For our irradiated materials, diffractograms were created from images taken at a magnification of 135kx. Distances from the center of the diffractograms to the center circle edge, first ring edge, and second ring edge were plotted. These data points were then used to produce the ratio from the ring edges to the central circle edge, which are shown in Table 2. As seen in Table 2, the ratio increases with irradiation dose, both for the samples irradiated at room temperature and those irradiated at 200°C, indicating densification of the BAM-11 alloy with ion irradiation. This observation matches up well with the slight increase in Young's modulus observed in the samples irradiated at 200°C but is at odds with the slight decrease in Young's modulus observed in the room temperature samples.

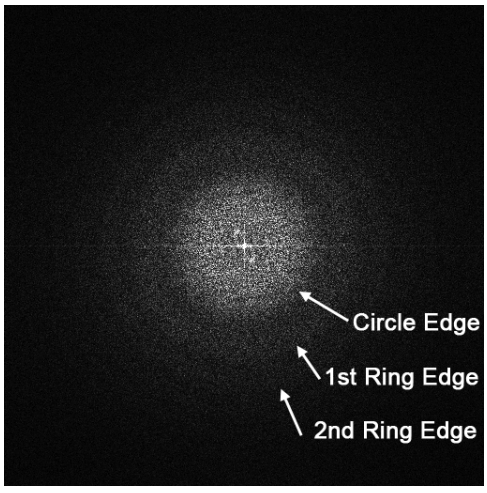

Figure 3. Diffractogram of the BAM-11 specimen irradiated to 1.0 dpa at 200°C. Circle, first ring, and second ring edges are shown.

Table 2. Summary of diffractogram measurements on unirradiated and irradiated BAM-11 specimens.

	Ratio from 1st Ring Edge to Circle Edge	Ratio from 2nd Ring Edge to Circle Edge
Unirradiated	1.54	1.94
0.1 dpa, RT	1.62	2.15
1.0 dpa, RT	1.76	2.24
0.1 dpa, 200C	1.55	2.01
1.0 dpa, 200C	1.65	2.10

CONCLUSIONS

After irradiation with 3 MeV Ni^+ ions to dose levels of 0.1 and 1.0 dpa at room temperature and 200°C, amorphous BAM-11 bulk metallic glass specimens were found to exhibit no observable changes in microstructure and only minor (less than ~10%) changes in mechanical properties. A slight degree of sample densification following irradiation, as seen via changes in Young's modulus and diffractogram data, was also observed.

Overall, the favorable constitutive response of BAM-11 following irradiation to low fluence levels indicates that the alloy may have applications as a structural material in nuclear applications, albeit only in low temperature scenarios where the alloy stays below its glassy transition temperature. However, studies of bulk metallic glasses in general seem to show a strong correlation between total dose and irradiation-induced crystallization, as shown in Table 1. For many fusion applications, bulk metallic glasses would likely undergo neutron irradiation to levels of 10-100 dpa. Therefore, further work is needed to understand the response of BAM-11 to very high fluence levels, and neutron-irradiation studies are also needed to help understand how the material would behave in a nuclear environment.

REFERENCES

[1] W. Klement, R. H. Wilens, and P. Duwez, *Nature* **187** (1960) 869-870.
[2] R. W. Cahn, *Nature* **341** (1989) 183-184.
[3] P. Chaudhari and D. Turnbull, *Science* **199** (1978) 11-21.
[4] A. L. Greer, *Science* **267** (1995) 1947-1953.
[5] W. J. Weber, R. C. Ewing, C. A. Angell, G. W. Arnold, A. N. Cormack, J. M. Delaye, D. L. Griscom, L. W. Hobbs, A. Navrotsky, D. L. Price, A. M. Stoneham, and M. C. Weinberg, *J. Mater. Res.* **12** (1997) 1946-1978.
[6] X. Mei, B. Wang, C. Dong, F. Gong, Y. Wang, and Z. Wang, *Nucl. Instrum. Methods Phys. Res. B* **307** (2013) 11-15.
[7] A. Inoue, *Acta Mater.* **48** (2000) 279-306.
[8] W. L. Johnson, *MRS Bulletin* **24** (1999) 42-56.
[9] M. Sorescu, *J. Alloys Compd.* **284** (1999) 232-236.

[10] J. Carter, E. G. Fu, G. Bassiri, B. M. Dvorak, N. D. Theodore, G. Xie, D. A. Lucca, M. Martin, M. Hollander, X. Zhang, and L. Shao, *Nucl. Instrum. Methods Phys. Res. B* **267** (2009) 1518-1521.
[11] M. Iqbal, J. I. Akhter, Z. Q. Hu, H. F. Zhang, A. Qayyum, and W. S. Sun, *J. Non-Cryst. Solids* **353** (2007) 2452-2458.
[12] W. D. Luo, B. Yang, and G. L. Chen, *Scripta Mater.* **64** (2011) 625-628.
[13] M. Myers, E. G. Fu, M. Myers, H. Wang, G. Xie, X. Wang, W.-K. Chu, and L. Shao, *Scripta Mater.* **63** (2010) 1045-1048.
[14] Y. Z. Yang, P. J. Tao, G. Q. Li, Z. X. Mu, Q. Ru, Z. W. Xie, and X. C. Chen, *Intermetallics* **17** (2009) 722-726.
[15] Z. Hu, Z. Zhao, Y. Hu, J. Xing, T. Lu, and B. Wei, *Mater. Res.* **15** (2012) 713-717.
[16] N. Kawasegi, N. Morita, S. Yamada, N. Takano, T. Oyama, K. Ashida, J. Taniguchi, I. Miyamoto, S. Momota, and H. Ofune, *Appl. Phys. Lett.* **89** (2006) 143115.
[17] Y. Fukumoto, A. Ishii, A. Iwase, Y. Yokoyama, and F. Hori, *J. Phys.: Conf. Ser.* **225** (2010) 012010.
[18] N. Onodera, A. Ishii, Y. Fukumoto, A. Iwase, Y. Yokoyama, and F. Hori, *Nucl. Instrum. Methods Phys. Res. B* **282** (2012) 1-3.
[19] R. Raghavan, K. Boopathy, R. Ghisleni, M. A. Pouchon, U. Ramamurty, and J. Michler, *Scripta Mater.* **62** (2010) 462-465.
[20] R. Raghavan, B. Kombaiah, M. Dobeli, R. Erni, U. Ramamurty, and J. Michler, *Mater. Sci. Eng. A* **532** (2012) 407-413.
[21] C. T. Liu, L. Heatherly, D. S. Easton, C. A. Carmichael, J. H. Schneibel, C. H. Chen, J. L. Wright, M. H. Yoo, J. A. Horton, and A. Inoue, *Metall. Mater. Trans. A* **29A** (1998) 1811-1820.
[22] J. F. Ziegler, J. P. Biersack, and U. Littmark. The Stopping and Range of Ions in Solids, Pergamon Press, New York (1985). Also see: http://www.srim.org.